Electronic Materials Letters, Vol. 6, No. 1 (2010), pp. 23-26
DOI: 10.3365/eml.2010.03.23 Published 31 March 2010

Elastic Modulus of Amorphous $Ge_2Sb_2Te_5$ Thin Film Measured by Uniaxial Microtensile Test

Yunjung Choi and Young-Kook Lee*

Department of Materials Science and Engineering, Yonsei University,
134 Shinchon-dong, Seodaemun-gu, Seoul 120-749, Korea

The elastic property of an amorphous $Ge_2Sb_2Te_5$ thin film was investigated by uniaxial microtensile test using amorphous $Ge_2Sb_2Te_5$ films deposited on both sides of a polyimide substrate. The elastic modulus of the amorphous $Ge_2Sb_2Te_5$ thin film was determined by the rule of mixture as 20.2 ± 1.3 GPa, comparable to that converted from the biaxial modulus measured by wafer curvature measurements. However, the elastic modulus measured by nanoindentation tests is higher than those measured by uniaxial microtensile test and by wafer curvature measurements, as the viscoelastic recovery component of the amorphous $Ge_2Sb_2Te_5$ film is not implied in the initial slope of the unloading curve in nanoindentation tests.

Keywords: microtensile test, Young's modulus, viscoelasticity, amorphous $Ge_2Sb_2Te_5$ film

1. INTRODUCTION

A cell of phase-change random access memory (PRAM) is a resistor consisting of chalcogenide materials that typically include a Ge-Sb-Te compound, where the phase constitutes the information bit depending on the presence of a crystalline or an amorphous phase.[1] During the PRAM operation, thermal stress caused by a temperature gradient and the differences in the thermal expansion coefficients between the phase change materials and surrounding materials is introduced, and phase transformation stress is also occurred.[2-4] These stresses are closely related to the failure and durability (cyclability) of PRAM cells.

For these reasons, the mechanical properties of Ge-Sb-Te thin films have been investigated using various experimental techniques, such as wafer curvature measurements,[3,5,6] nanoindentation tests,[6-8] and Brillouin light scattering.[9] However, uniaxial microtensile tests of Ge-Sb-Te thin films have yet to be reported, most likely due to the difficulty in specimen fabrication inherent in Ge-Sb-Te thin films, although microtensile tests of thin films of gold, silicon, and aluminum[10-12] have been conducted. In this study, therefore, the Young's modulus of an amorphous $Ge_2Sb_2Te_5$ (*a*-GST) thin film was investigated by uniaxial microtensile test using a newly devised specimen. This was then compared with the reported values as determined by the wafer curvature and by nanoindentation measurements.

*Corresponding author: yklee@yonsei.ac.kr

2. EXPERIMENTAL PROCEDURE

Figure 1(a) shows the geometry and dimensions of the tensile specimen used here. A polyimide film (DuPont Kapton® Type HN) with a thickness of 25 mm and with high thermal durability was used as a substrate. $Ge_2Sb_2Te_5$ thin films were deposited on one side of the polyimide substrate and then on the reverse side, without an interlayer between the film and substrate,[13] at room temperature by DC-magnetron sputtering using a stoichiometric target. The base pressure was 6.0×10^{-8} Torr and the process pressure during the sputtering process in Argon ambient was 1.0×10^{-3} Torr. The sputtering

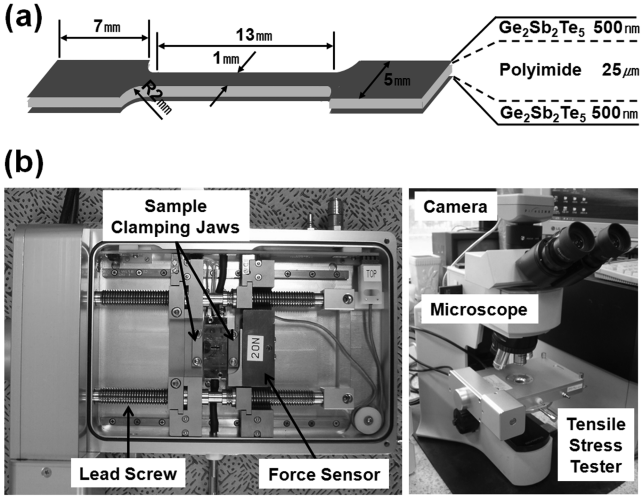

Fig. 1. (a) Geometry and dimensions of a tensile specimen and (b) photograph of a microtensile tester.

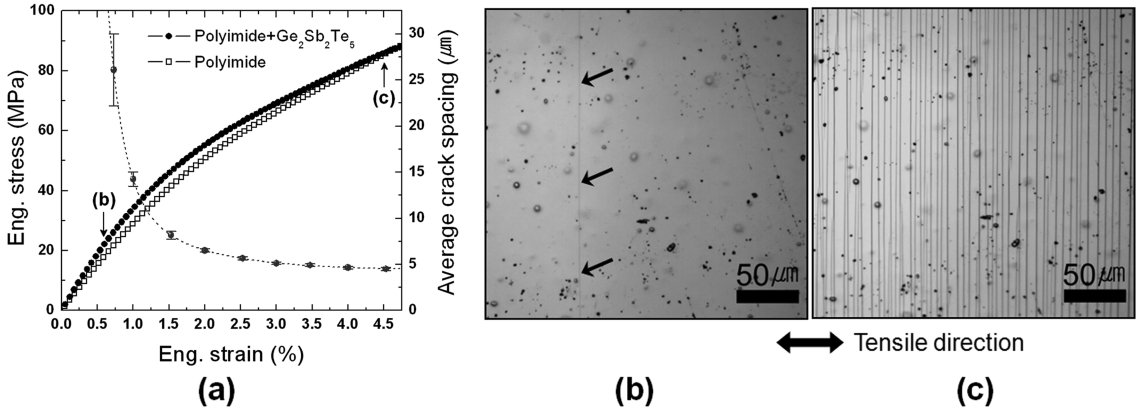

Fig. 2. (a) Engineering stress-strain curves of polyimide and composite (polyimide and amorphous $Ge_2Sb_2Te_5$) films deformed at a constant tensile speed of 1.0 mm/s, and average crack spacing between neighboring cracks in the direction parallel to tensile axis as a function of strain (gray circle). (b) and (c) are the surface images of the amorphous $Ge_2Sb_2Te_5$ film deformed by 0.6% and 4.5%, respectively. The micro-cracks are observed vertically to tensile direction.

power was 200 W. The chemical composition and crystal structure of the as-deposited films were measured by Auger electron spectroscopy and by X-ray diffraction, respectively. The chemical composition was determined to be $Ge_{24.5}Sb_{22.9}Te_{52.6}$ and the structure was found to be amorphous. The *a*-GST film thickness of each side of the substrate was 500 nm, as determined by a scanning electron microscope.

A microtensile tester (Linkam, TST 350) is shown in Fig. 1(b). Both ends of the tensile specimen were gripped by jaws which were 15 mm apart. A load cell with a capacity of 20 N was used to measure the applied force. The tensile tests were carried out at constant speeds of 1.0 mm/s, 1.5 mm/s, and 2.0 mm/s at room temperature. *In-situ* observations of the film surface were made using an optical microscope during the tensile tests.

3. RESULTS AND DISCUSSION

Figure 2(a) shows the engineering stress-strain curves of both a polyimide film and a composite film consisting of polyimide and *a*-GST. Three polyimide films and three composite films were tested at each tensile speed, and the relationship between the stress and strain was found to be generally reproducible under each condition. There was no effect of the tensile speed on the Young's modulus of the polyimide (E_s) in the range of 1.0 mm/s to 2.0 mm/s. However, the yield stress of polyimide, which was determined using an offset strain of 0.2%, changed slightly from 55 to 60 MPa as the tensile speed increased from 1.0 mm/s to 2.0 mm/s.

The composite film exhibited a higher Young's modulus and greater flow stress compared to the polyimide film. However, because the *a*-GST thin film was very brittle, micro-cracks were generated in this film as it underwent tensile deformation. As shown in Fig. 2(b), a crack formed vertically in the tensile direction at 0.6% strain; with additional strain, the number of cracks increased constantly (Fig. 2(c)). Cracks traversed the width of the specimen. The dependence of the average crack spacing between neighboring cracks on the strain is also shown in Fig. 2(a). After the onset of cracking at 0.6% strain, the average crack spacing decreased rapidly as the strain increased to approximately 1.5% and then gradually decreased further to approximately 5 μm. Finally, some fragments of the *a*-GST thin films were detached from the substrate during the tensile tests.

The stress-strain curve of the *a*-GST was converted by applying the following rule of mixture[14] to the stress-strain curves of the polyimide and composite films. This is shown in Fig. 3.

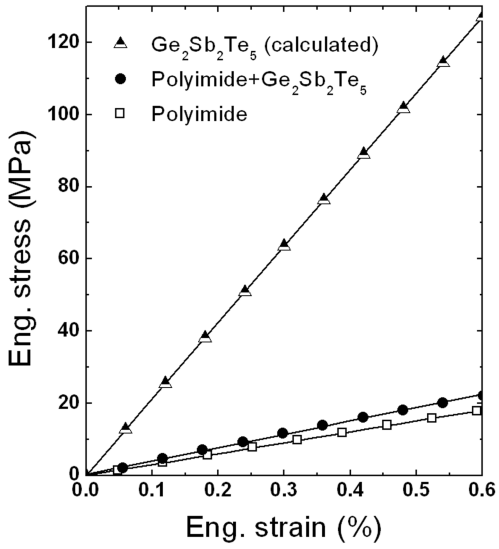

Fig. 3. The measured stress-strain curves of polyimide and composite (polyimide and amorphous $Ge_2Sb_2Te_5$) films and the calculated stress-strain curve of pure amorphous $Ge_2Sb_2Te_5$. The tensile speed was 1.0 mm/s.

$$\sigma_c = F_c/WT = \sigma_f A_f + \sigma_s A_s \quad (1)$$

Here, σ, F, W, and T are the stress, force, total width and total thickness of the sample, respectively. A is the cross-sectional area fraction. Also in the equation, f, s, and c refer to the a-GST, polyimide, and composite film, respectively. The elastic modulus was determined to be the slope of the stress-strain curve at a strain range of 0% to 0.6%. The Young's moduli of the polyimide substrate (E_s) and composite film (E_c) are 3.0 ± 0.1 GPa and 3.7 ± 0.1 GPa, respectively. The cross-sectional area fractions of the a-GST and polyimide, A_f and A_s, are 1/26 and 25/26, respectively. Therefore, the Young's modulus of the a-GST (E_f) is 20.2 ± 1.3 GPa.

The Young's modulus of the a-GST thin film determined by uniaxial microtensile test is compared with earlier measurements by different experimental techniques in Table 1.

In the wafer curvature measurement of the elastic deformation of the thin films, the change in the film stress $\Delta\sigma$ with the temperature T is proportional to the biaxial modulus of the film M_f and the difference in the thermal expansion coefficient α of the substrate and the film ($\Delta\sigma/\Delta T = M_f(\alpha_s - \alpha_f)$). The biaxial modulus ($M_f = E_f / (1 - \nu_f)$) is related to the Young's modulus with the Poisson's ratio, ν_f. However, an accurate ν_f value of $Ge_2Sb_2Te_5$ thin film has not been reported thus far. Hence, it is simply assumed to be 0.3.[5,6] The E_f value measured by the uniaxial microtensile tests in this study is coincident with the Young's modulus converted from the M_f value assuming ν_f is 0.3, as shown in Table 1. The Young's modulus of a-GST thin films with the thickness range of 300 nm to 1000 nm[5,6] was constant.

However, the E_f values measured by the nanoindentation tests were much greater than those measured by the uniaxial tensile and the biaxial bending tests. If the a-GST thin film and the substrate do not have a similar Young's modulus and Poisson's ratio, the substrate can affect the elastic property of the a-GST film during the nanoindentation tests.[15] In both nanoindentation tests shown in Table 1, a silicon wafer (E = 165 GPa, ν = 0.27)[16] was used as the substrate. To minimize the influence of the silicon substrate on the E_f value, the E_f data obtained in the shallow indentation depth region were averaged, and King's model[15,17] including a substrate compliance term was applied for the E_f value. In spite of these corrections, the nanoindentation test continued to result in a high E_f value, possibly due to the differences in the elastic recovery behavior of amorphous materials compared to that of crystalline materials.

Generally, the deformation of a solid consists of three components: reversible elastic deformation that recovers instantaneously upon unloading, viscoelastic deformation that recovers with time, and irreversible viscoplastic deformation. For crystalline materials, the viscoelastic strain is negligible compared to the viscoplastic strain, especially near room temperature. For amorphous materials, the viscoelastic contribution is a major part of the deformation. The viscoelasticity is caused by time-dependent atomic diffusion inside short-range ordered amorphous materials.[14]

The elastic and viscoelastic deformations occur in the a-GST thin films at low elastic stress levels in the wafer curvature measurements[5] and microtensile tests. For the nanoindentation test, during the loading, elastic, viscoelastic, and viscoplastic deformations were induced. Upon unloading, elastic recovery promptly occurred while the viscoelastic recovery exhibited time-dependency.[18,19]

The E_f values measured by nanoindentation in Table 1 were determined by the slope of the initial part of the load (P) – the indentation depth (h) curve obtained during unloading without the contribution of the viscoelastic recovery process. Therefore, the initial slope of the unloading curve (dP/dh) is steeper than that accompanying the viscoelastic recovery component, leading to a high E_f value.

4. CONCLUSIONS

The Young's modulus E_f of an amorphous $Ge_2Sb_2Te_5$ thin film was investigated via uniaxial microtensile test. The measured E_f value was 20.2 ± 1.3 GPa, which is coincident with that converted from the biaxial modulus measured by the wafer curvature measurements. However, the E_f value measured by nanoindentation is much larger than those assessed in a uniaxial tensile test and/or by wafer curvature measurements. Hence, this work demonstrates a useful method of measuring the mechanical properties of thin films without the need for a complex fabrication procedure for microtensile test specimens.

Table 1. Comparison of elastic modulus of amorphous $Ge_2Sb_2Te_5$ thin film

Reference	Test method	Substrate	Film thickness (nm)	Young's modulus (GPa)	Biaxial modulus (GPa)
This work	Uniaxial microtensile	Polyimide	500	20.2±1.3	-
Kalb[5]	Curvature measurement	Si (100), Al_2O_3	1000	19.3*	27.6±4.7
Park[6]	Curvature measurement	Si (100), Glass	300	20.7*	29.5±1.9
Park[6]	Nanoindentation	Silicon	300	33.9±0.7	-
Hong[7]	Nanoindentation	Silicon	400	31-35	-

*The values were converted from the measured biaxial modulus values.

ACKNOWLEDGMENT

This work was supported by Next-generation growth engine project of the Ministry of Knowledge Economy.

REFERENCES

1. S. R. Ovshinsky, *Phy. Rev. Lett.* **21**, 1450 (1968).
2. T. Gille, J. Lisoni, L. Goux, K. De Meyer, and D. J. Wouters, *Proc. Thermal, Mechanical and Multi-Physics Simulation Experiments in Micro/Nanoelectronics and Systems Conf.* (ed., L. J. Ernst), p.1, EuroSimE, London, GB (2007).
3. T. P. L. Pedersen, J. Kalb, W. K. Njoroge, D. Wamwangi, M. Wuttig, and F. Spaepen, *Appl. Phys. Lett.* **79**, 3597 (2001).
4. A. Pirovano, A. Redaelli, F. Pellizzer, F. Ottogalli, M. Tosi, D. Ielmini, A. L. Lacaita, and R. Bez, *IEEE Trans. Dev. Mater. Reliab.* **4**, 422 (2004).
5. J. Kalb, F. Spaepen, T. P. L. Pedersen, and M. Wutting, *J. Appl. Phys.* **94**, 4908 (2003).
6. I.-M. Park, J.-K. Jung, S.-O. Ryu, K.-J. Choi, B.-G. Yu, Y.-B. Park, S. M. Han, Y.-C. Joo, *Thin Solid Films*, **517**, 848 (2008).
7. S.-D. Hong, S.-M. Jeong, S.-S. Kim, and H.-L. Lee, *J. Kor. Ceram. Soc. (in Korean)* **42**, 326 (2005).
8. C.-A. Jong, W. Fang, C.-M. Lee, and T.-S. Chin, *Jpn. J. Appl. Phys.* **40**(Part 1, No. 5A), 3320 (2001).
9. T. Blachowicz, M. G. Beghi, G. Guntherodt, B. Beschoten, H. Dieker, and M. Wuttig, *J. Appl. Phys.* **102**, 093519 (2007).
10. S. W. Han, H. W. Lee, H. J. Lee, J. Y. Kim, J. H. Kim, C. S. Oh, and S. H. Choa, *Curr. Appl. Phys.* **6S1**, e81 (2006).
11. C.-S. Oh, H.-J. Lee, S.-G. Ko, S.-W. Kim, and H.-G. Ahn, *Sens. Actuators A* **117**, 151 (2005).
12. C. Malhaire, M. Ignat, K. Dogheche, S. Brida, C. Josserond, and L. Debove, *Proc. Solid-State Sensors, Actuators and Microsystems Conf.* (ed., G. Delapierre), p.623, Transducers&Eurosensors, Lyon, France (2007).
13. G. Geandier, P. -O. Renault, E. Le Bourhis, Ph. Goudeau, D. Faurie, C. Le Bourlot, Ph. Djemia, O. Castelnau, and S. M. Cherif, *Appl. Phys. Lett.* **96**, 041905 (2010).
14. T. H. Courtney, *Mechanical Behavior of Materials, 2nd ed.*, p. 247, 354, McGraw-Hill, Singapore (2000).
15. R. Saha and W. D. Nix, *Acta Mater.* **50**, 23 (2002).
16. T. Chudoba, N. Schwarzer, and F. Richter, *Surf. Coat. Technol.* **127**, 9 (2000).
17. R. B. King, *Int. J. Solids Struct.* **23**, 1657 (1987).
18. A. H. W. Ngan and B. Tang, *J. Mater. Res.* **17**, 2604 (2002).
19. J. Menčík, G. Rauchs, J. Bardon, and A. Riche, *J. Mater. Res.* **20**, 2660 (2005).